Photochemistry and Photobiology, 2021, 97: 1391–1396

Special Issue Research Article

Chemoselective Photoreaction of Enamides: Divergent Reactivity towards [3+2]-Photocycloaddition *vs* Paternò–Büchi Reaction†

Sunil Kumar Kandappa[1,3], Elango Kumarasamy[1,4], Ravichandranath Singathi[1], Lakshmy Kannadi Valloli[1], Angel Ugrinov[2] and Jayaraman Sivaguru[1]*

[1]Center for Photochemical Sciences and Department of Chemistry, Bowling Green State University, Bowling Green, OH, USA
[2]Department of Chemistry and Biochemistry, North Dakota State University, Fargo, ND, USA
[3]Department of Chemistry, University of Southern California, Los Angeles, CA, USA
[4]Conamix Inc, Ithaca, NY, USA

Received 18 June 2021, revised 14 July 2021, accepted 16 July 2021, DOI: 10.1111/php.13489

ABSTRACT

Photoreaction of enamides tethered to a phenyl ketone leads to either [3+2]-photocycloaddition or Paternò–Büchi reaction. This divergence in chemical reactivity originating from the same excited state was dependent on the reaction temperature. At low temperatures the Paternò–Büchi reaction was preferred, whereas at higher temperatures there was preference toward formation of [3+2]-photoproduct.

INTRODUCTION

Unlike ground-state (thermal) reaction, photoreaction involves the excited state where short lifetime of reactive species (singlet or triplet state) dictates the trajectory of reaction (1). Leveraging the outcome of photoreactions to access the desired product often involves a change in the nature of the excited states (2–6). Inoue, Mori and coworkers explored the effect of temperature on enantioselectivity/diastereoselectivity in photoreaction where product chirality can be completely inverted upon changing the temperature (7–9). Previous studies from our group also showcased the effect of temperature on enantioselectivity in photochemical 4π-ring closure of axially chiral 2-pyridones bearing the hydroxyl group that can form H-bonding interaction (10). Building on these precedents, we were interested in exploring the influence of reaction temperature on product chemoselectivity among well-established photochemical transformations. In this report, we disclose a temperature-dependent chemoselective transformations involving enamides **1a,b** leading to either Paternò–Büchi product **2a,b** or the [3+2]-photoproduct **3a,b** respectively (Scheme 1). This new strategy provides a complementary platform to access products obtained through [3+2]-photocycloaddition reactions (11–13).

MATERIALS AND METHODS

All commercially obtained reagents/solvents were used as received; chemicals were purchased from Alfa Aesar®, Sigma-Aldrich®, Acros organics®, Mallinckrodt, TCI America® and Oakwood® Products were used as received without further purification. Unless stated otherwise, reactions were conducted in oven-dried glassware under nitrogen atmosphere. Details related to the analytical and photophysical methods employed are provided in the Supporting Information. The enamides were synthesized by established literature procedures (14). Characterization of the photoproducts is provided in the Supporting Information. For photophysical studies, spectrophotometric grade solvents (Sigma-Aldrich®) were used whenever necessary, unless or otherwise mentioned. UV quality fluorimeter cells (with range until 190 nm) were purchased from Luzchem®. Absorbance measurements were performed using a Cary 300 UV-vis spectrophotometer. Time-resolved phosphorescence measurements were recorded on an FLS 1000 Photoluminescence Spectrometer (Edinburgh Instruments). Phosphorescence lifetime (τ_p) were performed at 77 K. Ethanol samples solutions in 3-mm quartz tubes (inner diameter) were frozen in a liquid nitrogen Dewar (77 K) and excited with a pulsed microsecond lamp for phosphorescence emission and lifetime measurements.

General irradiation procedure. A N_2 saturated solution of phenyl ketone derivative **1a-b** (concentration: 1 mg/1 mL or 2.7-3.0 mM) and xanthone photosensitizer (20 mol%) in dry acetonitrile (MeCN) was irradiated in a Rayonet reactor equipped with ~350 nm light bulbs until the reaction was complete as monitored by the ^{1}H-NMR spectroscopy and by thin layer chromotography (TLC). Large-scale photoreactions were performed as batches at the same concentration (8 × 10 mL test tubes per batch) using a merry-go-round apparatus. After completion of the reaction, the solvent was evaporated under reduced pressure and the residue was purified by CombiFlash to obtain the pure product. ^{1}H-NMR spectroscopy of the crude reaction mixture was used to monitor the reaction. Low-temperature reaction (−40°C and −5°C) was performed using an immersion cooler. Solution of reactants in a Pyrex test tube was kept in an acetone bath inside the Rayonet reactor with an immersion cooler set at the required temperature. An acetonitrile bath was maintained in a Pyrex jacket, and proper care was taken to ensure that temperature was above the melting point of acetonitrile. Further precautions were taken to avoid the formation of ice on the walls of the vessel that would prevent the penetration of light into the reaction mixture. The reaction mixture in the Pyrex test tube was allowed to reach equilibrium temperature of the bath (at least for 15 min) before the irradiation. High-temperature reaction was performed in a water bath placed over a hot plate maintained at the required temperature. A Pyrex test tube containing degassed solution of the reaction mixture was immersed in the water bath in a Pyrex beaker. This setup was placed inside the Rayonet reactor for irradiation.

RESULTS AND DISCUSSION

Although, there are plethora of literature reports on the effect of temperature on enantioselectivity or diastereoselectivity in a photochemical reaction (15,16), there are very few reports of product selectivity on temperature effects originating from the same

*Corresponding author email: sivagj@bgsu.edu (Jayaraman Sivaguru)
†This article is part of a Special Issue celebrating the career of Dr. Edward Clennan

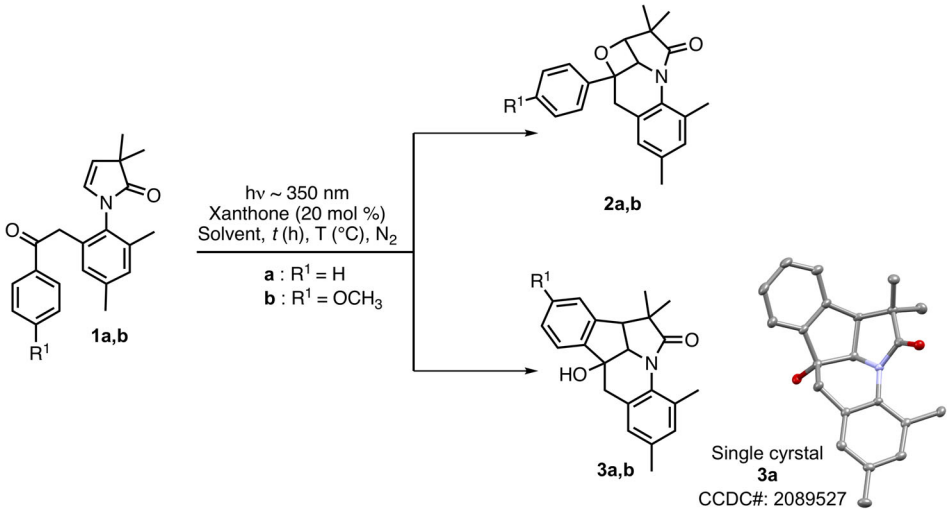

Scheme 1. Chemoselective photoreactivity of enamide **1**.

excited state (17–19). We had previously investigated the photoreaction of enamides, leading to transposed Paternò–Büchi reaction (14). During the course of our investigation, we observed a minor uncharacterized side product when the reaction was performed at room temperature. We were able to minimize or eliminate this uncharacterized side product by performing the reaction at low temperatures (−30°C), leading to the formation of a Paternò–Büchi product in high yield (14). Intrigued by this uncharacterized side product that was observed at room temperature, we initiated a detailed investigation to characterize this side product. First, we performed photoreaction of **1a** in acetonitrile with xanthone as the photosensitizer at room temperature using ~350 nm light using a Rayonet reactor. After 5 h irradiation, the reaction mixture was concentrated, and the products were analyzed by various analytical techniques. Detailed analysis of isolated products revealed that in addition to our Paternò–Büchi product **2a** (observed as major product at low temperature) (14), a new [3+2]-photoproduct **3a** was also observed (total isolated yield of **2a** = 36% and **3a** = 18% at 25°C). Single-crystal XRD analysis unambiguously confirmed the structure of [3+2]-photoproduct **3a** (Scheme 1).

To investigate chemoselectivity during the photocatalyzed reaction of **1a**, we systematically varied the reaction temperature from −40°C to +70°C in acetonitrile (Table 1). The chemoselectivity between **2a** and **3a** was monitored (Fig. 1) using the proton resonances of the oxetane ring (highlighted in Fig. 1 as H_a) and the α-hydrogen in the tetrahydroquinoline ring (highlighted in Fig. 1 as H_b) as NMR handles. At −40°C, the ratio of **2a**:**3a** was 1:0.1 (Table 1; entry 1; Fig. 1A). Upon increasing the temperature to −5°C and 25°C, the ratio of **2a**:**3a** was 1:0.5 (Table 1; entry 2; Fig. 1B) and 1:0.8 (Table 1; entry 3; Fig. 1C), respectively. Carrying out the reaction at 70°C (below the boiling point of acetonitrile), the ratio of **2a**:**3a** was 1:1.1 (Table 1; entry 4 Fig. 1D). It is striking to note that the major product at higher temperature (70°C) was the [3+2]-photoproduct **3a**, whereas at lower temperatures, the major product was the Paternò–Büchi product **2a**.

To understand this chemoselective dichotomy originating from enamide chromophores, presumably from the same excited state (*vide infra*) (14) toward the formation of Paternò–Büchi *vs* [3+2]-photocycloaddition, we decided to investigate the photoreaction of **1b** that features a *para*-methoxy benzoyl substituent (Scheme 1). We specifically chose a *para*-methoxy substituent as we anticipated the lowest triplet excited state to be of ππ* character based on the similarities of a benzoyl part of enamides **1a** and **1b** with acetophenone and *para*-methoxy acetophenone, respectively (20,21). Previously, we had established that **1a** features lowest triplet excited state with a triplet energy (E_T) of ~73 kcal/mol above the ground state with a lifetime of 8 ms in EtOH at 77 K (14). The nature of the triplet excited state in **1a** was established as nπ* in character (similar to acetophenone) (14). On the other hand, time-resolved phosphorescence of **1b** in EtOH at 77 K showed a multiexponential decay with phosphorescence lifetimes ranging from 62 to 438 ms (Fig. 2 and Figure S6). Multiexponential lifetime in enamides is expected as it features two distinct chromophores (i.e. the alkene functionality in the five-membered ring and the carbonyl functionality associated with the *para*-methoxy benzoyl chromophore) in addition to having restricted bond rotations around the N-C(Aryl) bond, leading to atropisomerism (22). Prior work on dihydro-2-pyridones has shown that the enamide functionality has a lifetime of ~0.46 s highlighting a ππ* character (23). It is striking to note the similarities in the chromophore characteristics in **1b** and *para*-methoxy acetophenone. Based on the phosphorescence emission (Fig. 2) and lifetime measurements in **1b** (Figure S6), it is likely that the lowest excited state is of ππ* character (due to similarities with *para*-methoxy acetophenone functionality in

Table 1. Ratio of product distribution during photoreaction of enamide **1** at various temperatures.

Entry	Reactant	*T* (°C)	**2:3***
1	**1a**	-40	1:0.1
2	**1a**	-5	1:0.5
3	**1a**	25	1:0.8
4	**1a**	70	1:1.1
5	**1b**	25	1:0.3

*Monitored by ^{1}H-NMR spectroscopy. The proton resonances of the hydrogen in the oxetane ring and the α-hydrogen in the tetrahydroquinoline ring were used as NMR handles for deciphering the ratio of Paternò-Büchi product **2a** and the [3+2]-photoproduct **3a**, respectively.

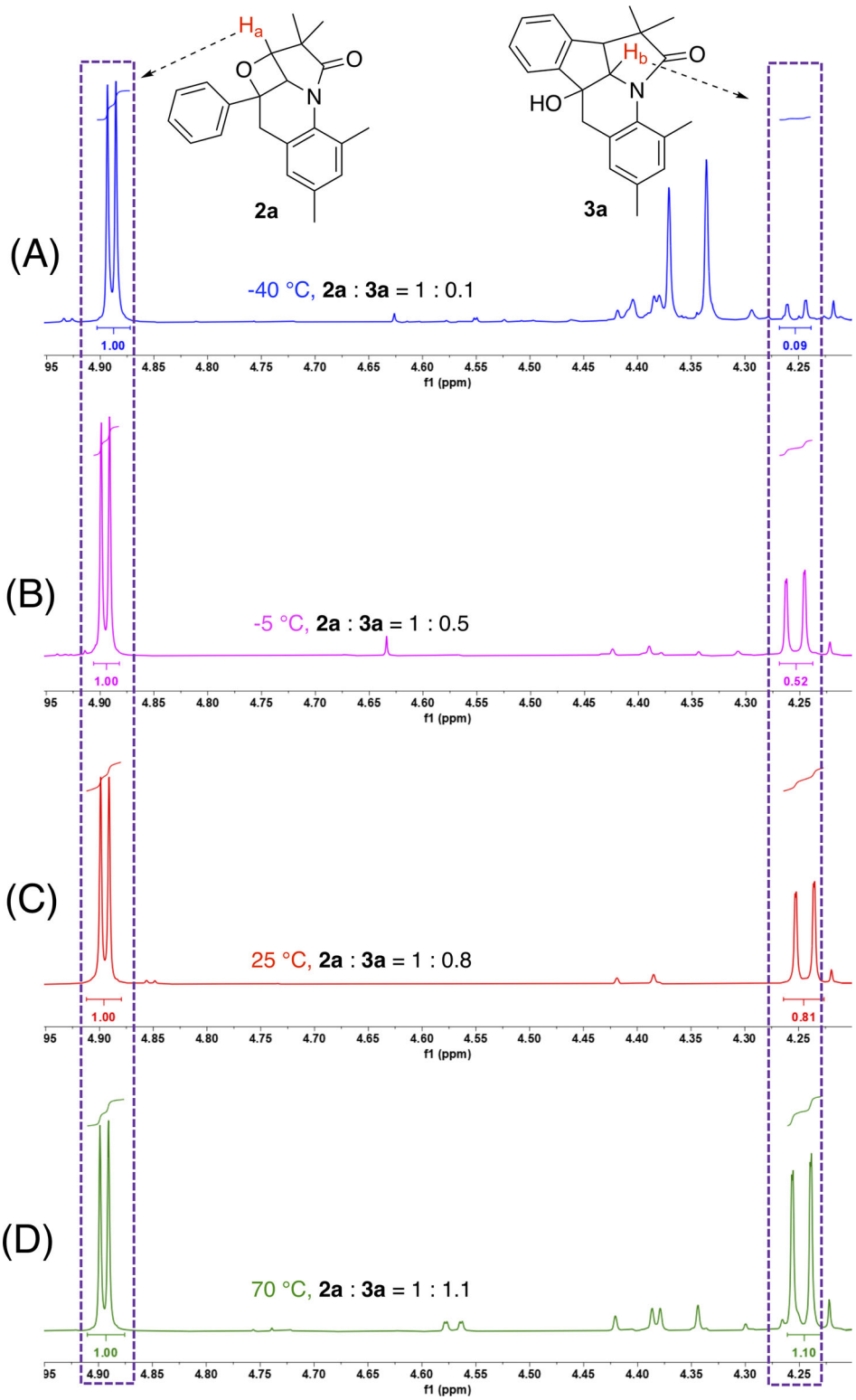

Figure 1. [1]H-NMR spectroscopic analysis of crude reaction mixture at −40°C (A), −5°C (B), 25°C (C) and 70°C (D) respectively. The proton resonances of the oxetane ring and the α-hydrogen in the tetrahydroquinoline ring were used as NMR handles for deciphering the ratio of Paternò–Büchi product **2a** and the [3+2]-photoproduct **3a**, respectively.

1b) (20,21). Similar to **1a**, photoreaction of **1b** was carried out under sensitized conditions at 25°C. Although we were able to observe the characteristic peaks for **2b** and **3b** (refer to Supporting Information; Figure S3) in the ratio of ~1:0.3, we were unable to isolate the product chromatographically owing to overlapping retention factors. Still the characteristic peaks of the

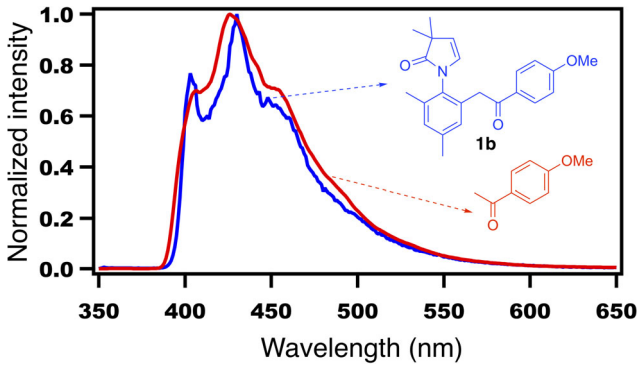

Figure 2. Phosphorescence spectra of enamide **1b** (blue, 4 mM) and 4-methoxy acetophenone (red, 4 mM) in ethanol glass at 77 K (λ_{Ex} = 315 nm; delay = 10 ms).

3b, albeit in low yields, show that the [3+2]-photocycloaddition is a divergent pathway in these types of chromophores.

The divergent behavior in enamide **1a** leading to different major photoproducts at low and high temperatures irrespective of starting from the same excited state can be mechanistically rationalized based on the excited-state reactivity of enamides (Scheme 2). Enamide **1a** features a triplet nπ* excited state (E_T ~73 kcal/mol with a lifetime of 8 ms) that can be accessed by sensitized irradiation with a xanthone sensitizer (E_T ~74 Kcal/mol) (14). Based on the established photochemical reactivity paradigm of carbonyl chromophores (24), the triplet nπ* of ketone functionality in **1a** reacts with the alkene unit to produce a 1,4-triplet biradical tBR-**1a**. This triplet biradical at low temperatures can intersystem cross to singlet biradical sBR-**1a** that subsequently form the Paternò–Büchi product **2a**. Upon increasing the temperature, the 1,4-triplet biradical tBR-**1a** can cyclize to form 1,4-triplet biradical tBR-**1a'**, which subsequently undergoes intersystem crossing, followed by re-aromatization to from the [3+2]-photoproduct **3a**. The fact that higher temperature is needed to access the [3+2]-photoproduct **3a** shows that the conversion of 1,4-triplet biradical tBR-**1a** to 1,4-triplet biradical tBR-**1a'** has an energy barrier. At low temperatures, the 1,4-biradical tBR-**1a** does not have sufficient energy to overcome this energy barrier, leading to the formation of the Paternò–Büchi product **2a** as the major product (**2a**:**3a** = 1:0.1; Table 1; entry 1; Fig. 1A). At high temperatures, the triplet 1,4-biradical tBR-**1a** can either undergo intersystem crossing, leading to **2a**, or overcome the energy to form

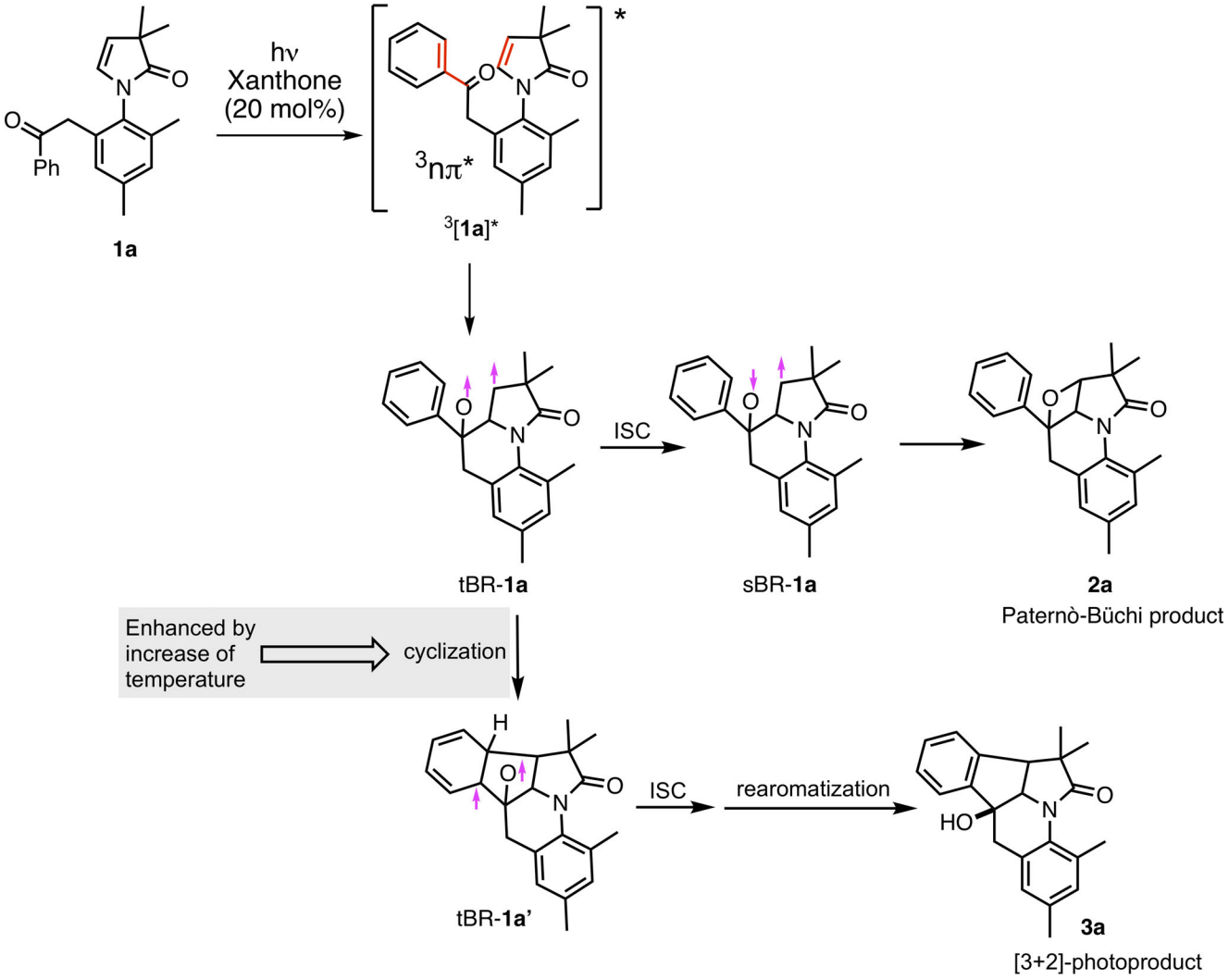

Scheme 2. Mechanistic rationale for the observed temperature dependent divergent reactivity.

the triplet 1,4-biradical tBR-**1a'** en route to the formation of the [3+2]-photoproduct **3a** (**2a**:**3a** = 1:1.1; Table 1; entry 4; Fig. 1D). The temperature dependence of chemoselectivity reflects the differentiation in the reaction rates of the triplet biradical tBR-**1a** (Scheme 2) from photoexcited enamides.

CONCLUSION

Our preliminary investigation establishes the formation of the [3+2]-product that is likely dictated by factors such as orientation of the orbitals, trajectory and accessibility of the radical center. This conjecture is also in line with the prediction by Tanko and coworkers (25) who hypothesized that the rates of hydrogen abstractions in reactive radicals are governed by entropic issues such as the factors listed before. Uncovering such new reaction trajectories from excited states offers a new avenue to develop novel photochemical processes providing access to unique and complex structural features in the photochemical products (26–28). Further efforts are underway in our laboratory to explore novel and unknown reactivity from the excited state(s) of organic chromophores.

Acknowledgements—The authors thank the National Science Foundation for generous support (CHE-1811795 and CHE-1955524). SK thanks the Center for Photochemical Sciences for the McMaster Fellowship. This manuscript is part of the special issue celebrating the retirement of our photochemistry colleague Prof. Edward Clennan. The manuscript was written through contributions of all authors. All authors have given approval to the final version of the manuscript. The authors thank Dr. Steffen Jockusch, Columbia University, New York, for insightful discussions and for help with photophysical experiments. Part of this work was carried out during the JS's association with North Dakota State University, Fargo, ND.

SUPPORTING INFORMATION

Additional supporting information may be found online in the Supporting Information section at the end of the article:

Chart S1. Chemical structure of photoproducts and its precursors used in the photoreactions.

Scheme S1. Synthesis of phenyl ketone derivative **1b**.

Scheme S2. Photoreaction of phenylketone derivative **1a** and **1b**.

Figure S1. Overlapped ^{1}H-NMR spectra of **2a** ([2+2]-photoproduct) and **3a** ([3+2]-photoproduct) depicting the proton resonance in the entire spectral range.

Figure S2. Expanded region of NMR spectra of crude reaction mixture depicting **2a** ([2+2]-photoproduct) and **3a** ([3+2]-photoproduct) at −40°C, −5°C, 25°C and 70°C.

Figure S3. Expanded region of NMR spectra of pure compound **1b, 2a, 3a,** and crude reaction mixture containing the mixture of **2b** and **3b**. Formation of **2b** confirmed with the doublet for proton resonance at ~ 4.94 ppm (as in pure **2a**-[2+2]-photoproduct). Formation of **3b** confirmed with the doublet for proton resonance at ~ 4.25 ppm (as in pure **3a-**[3+2]-photoproduct). Reaction mixture also shows unreacted starting material **1b** (on comparing the doublet for proton resonance at ~5.35 ppm for pure **1b** and the mixture of **2b** and **3b** in the crude reaction mixture).

Figure S4. Top: UV-Vis absorption spectra of 1 mM solution of **1b** in methyl cyclohexane (MCH). Bottom: Comparison of the UV-Vis absorption spectra of 1 mM solution of **1b** and 0.2 mM of Xanthone.

Figure S5. Top: Phosphorescence spectra of enamide **1b** (blue, 4 mM) and 4-methoxy acetophenone (red, 4 mM) in ethanol glass at 77 K (λ_{Ex} = 315 nm; delay = 10 ms).

Figure S6. Phosphorescence emission decay of **1b** (4 mM) measured at 77 K in ethanol glass excited at 315 nm using pulsed xenon lamp (0.125 Hz) with delay of 10 ms. The phosphorescence decay was monitored at 405 nm.

Figure S7. ^{1}H-NMR of 4-methoxy phenylketone derivative **1b**.

Figure S8. ^{13}C-NMR of 4-methoxy phenylketone derivative **1b**.

Figure S9. ^{1}H-NMR of [3+2]-photocycloaddition product **3a**.

Figure S10. ^{13}C-NMR of [3+2]-photocycloaddition product **3a**.

Figure S11. XRD structure of [3+2]-photocycloaddition product **3a**

REFERENCES

1. Turro, N. J., V. Ramamurthy and J. C. Scaiano (2010) A theory of molecular organic photochemistry. In *Modern Molecular Photochemistry of Organic Molecules*, pp. 319–382. University Science Books, Sausalito, CA.
2. Dauben, W. G., W. A. Spitzer and M. S. Kellogg (1971) Photochemistry of 4-methyl-4-phenyl-2-cyclohexenone. Effect of solvent on the excited state. *J. Am. Chem. Soc.* **93**, 3674–3677.
3. Uppili, S., S. Takagi, R. B. Sunoj, P. Lakshminarasimhan, J. Chandrasekhar and V. Ramamurthy (2001) Controlling the reactive state through cation binding: photochemistry of enones within zeolites. *Tetrahedron Lett.* **42**, 2079–2083.
4. Sunoj, R. B., P. Lakshminarasimhan, V. Ramamurthy and J. Chandrasekhar (2001) Configuration interaction and density functional study of the influence of lithium cation complexation on vertical and adiabatic excitation energies of enones. *J. Comput. Chem.* **22**, 1598–1604.
5. Ayitou, A.- J.-L. and J. Sivaguru (2011) Reactive spin state dependent enantiospecific photocyclization of axially chiral α-substituted acrylanilides. *Chem. Commun.* **47**, 2568–2570.
6. Ayitou, A.- J.-L., A. Clay, E. Kumarasamy, S. Jockusch and J. Sivaguru (2014) Enantiospecific photochemical 6π-ring closure of α-substituted atropisomeric acrylanilides - role of alkali metal ions. *Photochem. Photobiol. Sci.* **13**, 141–144.
7. Nagasaki, K., Y. Inoue and T. Mori (2018) Entropy-driven diastereoselectivity improvement in the paternò-büchi reaction of 1-naphthyl aryl ethenes with a chiral cyanobenzoate through remote alkylation. *Angew. Chem. Int. Ed.* **57**, 4880–4885.
8. Mori, T. (2020) Relevance of the entropy factor in stereoselectivity control of asymmetric photoreactions. *Synlett* **31**, 1259–1267.
9. Matsumura, K., T. Mori and Y. Inoue (2010) Solvent and temperature effects on diastereodifferentiating paternò-büchii reaction of chiral alkyl cyanobenzoates with diphenylethene upon direct versus charge-transfer excitation. *J. Org. Chem.* **75**, 5461–5469.
10. Kumarasamy, E., J. L. Jesuraj, J. N. Omlid, A. Ugrinov and J. Sivaguru (2011) Light-induced enantiospecific 4π ring closure of axially chiral 2-pyridones: enthalpic and entropic effects promoted by H-Bonding. *J. Am. Chem. Soc.* **133**, 17106–17109.
11. Gerard, B., G. Jones and J. A. Porco (2004) A biomimetic approach to the rocaglamides employing photogeneration of oxidopyryliums derived from 3-hydroxyflavones. *J. Am. Chem. Soc.* **126**, 13620–13621.
12. Gerard, B., S. Sangji, D. J. O'Leary and J. A. Porco (2006) Enantioselective photocycloaddition mediated by chiral brønsted acids: asymmetric synthesis of the rocaglamides. *J. Am. Chem. Soc.* **128**, 7754–7755.
13. Roche, S. P., R. Cencic, J. Pelletier and J. A. Porco (2010) Biomimetic photocycloaddition of 3-hydroxyflavones: synthesis and evaluation of rocaglate derivatives as inhibitors of eukaryotic translation. *Angew. Chem. Int. Ed.* **49**, 6533–6538.
14. Kumarasamy, E., R. Raghunathan, S. K. Kandappa, A. Sreenithya, S. Jockusch, R. B. Sunoj and J. Sivaguru (2017) Transposed Paternò-Büchi reaction. *J. Am. Chem. Soc.* **139**, 655–662.
15. Inoue, Y. (1992) Asymmetric photochemical reactions in solution. *Chem. Rev.* **92**, 741–770.

16. Inoue, Y. and V. Ramamurthy (2004) *Chiral Photochemistry*. Marcel Dekker, New York, NY.
17. Poon, T., J. Sivaguru, R. Franz, S. Jockusch, C. Martinez, I. Washington, W. Adam, Y. Inoue and N. J. Turro (2004) Temperature and solvent control of the stereoselectivity in the reactions of singlet oxygen with oxazolidinone-substituted enecarbamates. *J. Am. Chem. Soc.* **126**, 10498–10499.
18. Sivaguru, J., T. Poon, C. Hooper, H. Saito, M. Solomon, S. Jockusch, W. Adam, Y. Inoue and N. J. Turro (2006) A comparative mechanistic analysis of the stereoselectivity trends observed in the oxidation of chiral oxazolidinone-functionalized enecarbamates by singlet oxygen, ozone and triazolinedione. *Tetrahedron* **62**, 10647–10659.
19. Sivaguru, J., M. R. Solomon, H. Saito, T. Poon, S. Jockusch, W. Adam, Y. Inoue and N. J. Turro (2006) Conformationally controlled (entropy effects), stereoselective vibrational quenching of singlet oxygen in the oxidative cleavage of oxazolidinone-functionalized enecarbamates through solvent and temperature variations. *Tetrahedron* **62**, 6707–6717.
20. Kearns, D. R. and W. A. Case (1966) Investigation of singlet → triplet transitions by the phosphorescence excitation method. III. Aromatic ketones and aldehydes. *J. Am. Chem. Soc.* **88**, 5087–5097.
21. Wagner, P. J., A. E. Kemppainen and H. N. Schott (1973) Effects of ring substituents on the type II photoreactions of phenyl ketones. How interactions between nearby excited triplets affect chemical reactivity. *J. Am. Chem. Soc.* **95**, 5604–5614.
22. Kumarasamy, E., A.- J.-L. Ayitou, N. Vallavoju, R. Raghunathan, A. Iyer, A. Clay, S. K. Kandappa and J. Sivaguru (2016) Tale of twisted molecules. Atropselective photoreactions: taming light induced asymmetric transformations through non-biaryl atropisomers. *Acc. Chem. Res.* **49**, 2713–2724.
23. Kumarasamy, E. and J. Sivaguru (2013) Light-induced stereospecific intramolecular [2+2]-cycloaddition of atropisomeric 3,4-dihydro-2-pyridones. *Chem. Commun.* **49**, 4346–4348.
24. Turro, N. J., V. Ramamurthy and J. C. Scaiano (2010) Photochemistry of carbonyl compounds. In *Modern Molecular Photochemistry of Organic Molecules*, pp. 629–704. University Science Books, New York, NY.
25. Finn, M., R. Friedline, N. K. Suleman, C. J. Wohl and J. M. Tanko (2004) Chemistry of the t-Butoxyl radical: evidence that most hydrogen abstractions from carbon are entropy-controlled. *J. Am. Chem. Soc.* **126**, 7578–7584.
26. Kandappa, S. K., L. K. Valloli, S. Jockusch and J. Sivaguru (2021) Uncovering new excited state photochemical reactivity by altering the course of the de mayo reaction. *J. Am. Chem. Soc.* **143**, 3677–3681.
27. Wang, W., A. Clay, R. Krishnan, J. Lajkiewicz Neil, E. Brown Lauren, J. Sivaguru and A. Porco John (2017) Total syntheses of the isomeric aglain natural products foveoglin A and perviridisin B: selective excited-state intramolecular proton-transfer photocycloaddition. *Angew. Chem. Int. Ed.* **56**, 14479–14482.
28. Wen, S., J. H. Boyce, S. K. Kandappa, J. Sivaguru and J. A. Porco (2019) Regiodivergent photocyclization of dearomatized acylphloroglucinols: asymmetric syntheses of (−)-nemorosone and (−)-6-epi-garcimultiflorone A. *J. Am. Chem. Soc.* **141**, 11315–11321.